Soft Modes at the Critical End Point in the Chiral Effective Models

H. Fujii[a] and M. Ohtani[b]

[a]*Institute of Physics, University of Tokyo, Tokyo 153-8902*
[b]*Radiation Laboratory, RIKEN, Saitama 351-0198*

At the critical end point in QCD phase diagram, the scalar, vector and entropy susceptibilities are known to diverge. The dynamic origin of this divergence is identified within the chiral effective models as softening of a hydrodynamic mode of the particle-hole–type motion, which is a consequence of the conservation law of the baryon number and the energy.

§1. Introduction and Summary

Theoretical studies of QCD thermodynamics have been predicting rich phase structure in the plane of the temperature T and the chemical potential 3μ for baryon number, as discussed in the workshop, and there are heavy–ion programs now ongoing and planned in order to explore these new states of matter experimentally. Based on the lattice QCD results[1] as well as the effective model calculations[2]−[5] it is strongly argued that as one of the prominent features of the real diagram there exists a critical end point (CEP)[*] of the first–order transition line, which is reviewed by M.A. Stephanov[6]. Since it is a truly singular point, we expect clearer information of it from experiments. The basic property of CEP is the divergence of the susceptibilities of the baryon number and entropy densities as well as of the scalar density. Thus it is suggested that the fluctuations in the low–momentum pions and nucleons show anomalous behavior as functions of experimental parameters near CEP[7],[8]. Theoretical estimates indicate the possibility that the CEP gives still significant effects on these observables although the finiteness of the experimental geometry in space and time will round off the critical growth of these fluctuations[8],[9].

Near the critical point there will be at least one mode which becomes soft representing the criticality[10]. In this report we address the issue of the soft mode associated with CEP, which causes these critical divergences, within the Nambu–Jona-Lasinio model (NJL)[11],[12] and the time–dependent Ginzburg–Landau (TDGL) approach[12]. The correct identification of the soft mode associated with CEP is crucial to determine the time evolution of the critical fluctuations and to study the experimental signals.

So far the static properties of CEP have been investigated, where the underlying (approximate) chiral symmetry is usually emphasized. The effective potential with the scalar density σ as the order parameter, becomes flat around a nonzero equilibrium value of σ at CEP, reflecting the divergence of the scalar susceptibility.

---

[*] In condensed matter physics the term *critical end point* is used to indicate a different point where a critical line is truncated by meeting a first–order phase boundary.

This seemingly suggests the appearance of the gapless sigma mode there. We note here, however, that the baryon number and entropy susceptibilities diverge at CEP simultaneously. The scalar fluctuation is no more special than others once chiral symmetry is explicitly broken[*].

In this report we point out that the most important property of CEP is the divergent fluctuations of the conserved quantities such as the baryon number and the energy [12]. Since only the hydrodynamic mode contributes to the susceptibilities of these conserved quantities, the soft mode associated with CEP should have such a property and causes various divergences at CEP through the mixing. Within the NJL model calculation and the TDGL approach we show that this is indeed the case.

§2. Susceptibility as a spectral sum and its constraints

Divergence of the susceptibility implies that there appears at least one soft mode associated with the criticality. Since the susceptibility χ is obtained as a q–limit of the response function $\chi(\omega, \boldsymbol{q})$, which is analytic in the upper half plane of complex ω, one can express the susceptibility as a sum of the spectral strength over all frequencies:

$$\chi = \chi(0, \mathbf{0}^+) = \lim_{\boldsymbol{q}\to 0} \chi(0, \boldsymbol{q}) = \lim_{\boldsymbol{q}\to 0} \frac{\mathcal{P}}{\pi} \int_{-\infty}^{\infty} \frac{d\omega'}{\omega'} \mathrm{Im}\chi(\omega', \boldsymbol{q}), \qquad (2\cdot1)$$

where a ultra–violet regularization is understood if necessary. Spectral enhancement at vanishing ω is required to get the critical divergence because the spectral function $\rho(\omega, \boldsymbol{q}) = 2\mathrm{Im}\chi(\omega, \boldsymbol{q})$ itself is usually integrable.

Let us discuss the constraints on the spectral functions. First, in the second–order chiral transition with the massless quarks, the sigma mode becomes gapless so as to realize the manifest chiral symmetry in the spectrum together with the pion mode (see Ref. 14) for another possibility). In the typical NJL calculation [15], the spectral peak of the sigma meson ($\boldsymbol{q} = 0$) grows sharply and moves to $\omega = 0$ as the critical point is approached from the symmetric phase, which results in the divergent scalar susceptibility. At CEP with the finite quark mass, however, there is no symmetry reason to expect the gapless sigma meson.

The second constraint is a consequence of the conservation of the baryon number density and the energy density. The fluctuations of the conserved quantities are natural slow modes whose frequencies vanish in the long wavelength limit, and constitute a basis of hydrodynamics. For (e.g.,) the quark number density ρ there is a current $\boldsymbol{j}$ such that $\omega\rho - \boldsymbol{q}\cdot\boldsymbol{j} = 0$, which implies that $\omega \to 0$ as $\boldsymbol{q} \to \mathbf{0}$. A rephrasing of this fact is that the spectral function of the conserved density fluctuation is proportional to the delta function $\omega\delta(\omega)$ in the $\boldsymbol{q} \to 0$ limit [16), 12), 17)]. We call the spectrum with this property "hydrodynamic" in this report.

At CEP the quark number and entropy susceptibilities are divergent, to which only hydrodynamic spectrum contributes. This fact directly requires extra softness or critical slowing of a hydrodynamic mode near CEP to give these divergences.

---

[*] In studying the singularity of CEP, *approximate* chiral symmetry is at most secondary. The size of the critical region of CEP and the distance from TCP are different, interesting issues [13].
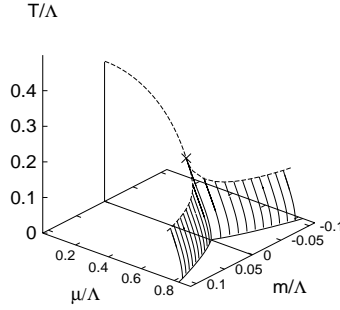
Fig. 1. Phase diagram of the NJL model in T–μ–m space. Three critical (dashed) lines meet at the tricritical point ×. The phase boundary (hatched) of the first-order transition forms a wing–like structure.

A remark here may be in order. The coupling with the hydrodynamic mode is the origin of the different limiting values of the response function at $(\omega, \boldsymbol{q}) = (0, \boldsymbol{0})$ [11]. In fact, the ω–limit of $\chi(\omega, \boldsymbol{q})$

$$\chi(0^+, \boldsymbol{0}) = \lim_{\omega \to 0} \frac{\mathcal{P}}{\pi} \int_{-\infty}^{\infty} \frac{d\omega'}{\omega' - \omega} \mathrm{Im}\chi(\omega', \boldsymbol{0}) \qquad (2\cdot2)$$

does not contain the contribution of the hydrodynamic mode, which is apparent from a formal relation $\omega\delta(\omega) = 0$.

§3. Nambu–Jona-Lasinio model [11]

3.1. *Phase diagram*

We study the simple Nambu–Jona-Lasinio model [16] $\mathcal{L} = \bar{q}(i\slashed{\partial} - m)q + g[(\bar{q}q)^2 + (\bar{q}i\gamma_5\tau^a q)^2]$ defined with the three-momentum cutoff Λ and with the coupling strength $g\Lambda^2 = 2.5$, within the mean field approximation. The effective potential for the scalar density σ yields

$$\Omega(T, \mu, m; \sigma) = -\nu \int \frac{d^3k}{(2\pi)^3}[E_{\boldsymbol{k}} - T\ln(1 - n_+) - T\ln(1 - n_-)] + \frac{1}{4g}\sigma^2, \quad (3\cdot1)$$

where $n_\pm = (e^{\beta(E\mp\mu)} + 1)^{-1}$, $E_{\boldsymbol{k}} = \sqrt{M^2 + \boldsymbol{k}^2}$, $M = m - \sigma$ and $\nu = 2N_f N_c = 2\cdot2\cdot3$.

The phase diagram in the T–μ–m space is shown Fig. 1. Within the symmetry plane $(m = 0)$, the chiral broken phase is separated from the symmetric phase by a critical line, on which the sigma meson mode is gapless. At temperatures below the *tricritical* point (TCP)[*] the boundary becomes the first–order line of three–phase coexistence [6]. As the explicit breaking term $m \neq 0$ is introduced and increased, this first–order line is lifted to form a wing–like structure. The densities of the scalar,

---

[*] Historically the point × is called tricritical because three critical lines meet there.
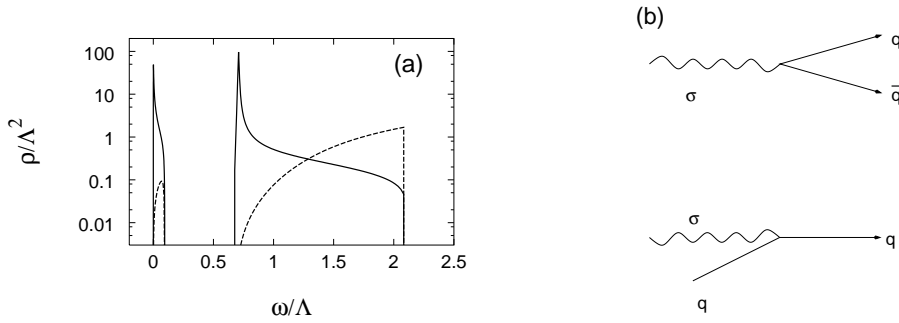
Fig. 2. (a) Spectral function in the scalar channel (solid) with $|\boldsymbol{q}|/\Lambda = 0.1$ at a CEP with $m/\Lambda = 0.01$. The free gas spectrum (dashed) is also shown for reference. (b) Typical processes contributing to the spectrum.

baryon number and entropy are discontinuous across this wing surface in general, and their susceptibilities contain the critical fluctuations at the edge of the wing[*].

3.2. *Spectrum in the scalar channel*

The collective motion of this model is generated through the (pseudo–) scalar interactions. The response functions in the scalar and vector channels are easily evaluated at the RPA level $(a, b = \mu, m)$:

$$\chi_{ab}(iq_4, \boldsymbol{q}) = \Pi_{ab}(iq_4, \boldsymbol{q}) + \Pi_{am}(iq_4, \boldsymbol{q}) \frac{1}{1 - 2g\Pi_{mm}(iq_4, \boldsymbol{q})} 2g\Pi_{mb}(iq_4, \boldsymbol{q}), \quad (3\cdot2)$$

where $\Pi_{ab}(iq_4, \boldsymbol{q})$ are the one–loop polarization functions calculated in the imaginary–time formalism. The real–time response function is obtained by the usual replacement $iq_4 \to q_0 + i\varepsilon$ in the final expression.

Let us first consider the scalar channel, in which collective mode is generated by the denominator in Eq. (3·2). In Fig. 2 (a) we present the spectral function $\rho(\omega, \boldsymbol{q}) = 2\mathrm{Im}\chi_{mm}(\omega, \boldsymbol{q})$ with $|\boldsymbol{q}|/\Lambda = 0.1$ at a CEP with $m/\Lambda = 0.01$. We clearly see a peak around $2M$ with $M/\Lambda = 0.331(\propto m^{1/5})$, corresponding to the sigma meson, which is interpreted as a collective excitation of the $\bar{q}q$ pairs (see Fig. 2 (b)). This sigma meson peak cannot give the critical divergence at CEP because it stays massive there. The peak is unphysically narrow in our model because we neglected the $\sigma \leftrightarrow \pi\pi$ coupling, which if included will broaden the width and decrease the threshold to $\sqrt{4m_\pi^2 + \boldsymbol{q}^2}$ with $m_\pi \sim m^{2/5} \neq 0$. The above conclusion will be unaltered in spite of this improvement.

There is another spectral peak in the spacelike–momentum region $(\omega < |\boldsymbol{q}|)$, which is generated by the collective absorption/emission of the scalar fluctuation by a quark or an anti–quark in medium (see Fig. 2 (b)). This type of motion is possible only in medium and called particle–hole (p–h) excitation, especially at zero temperature. The excitation energy of this motion is kinematically soft; $\omega \sim$

---

[*] In the vicinity of the critical lines except for TCP, the mean field approximation is known to break down due to large fluctuations. Furthermore, in the chiral broken phase with $m = 0$ the pionic fluctuation is the most important. We neglected these fluctuations in this work.
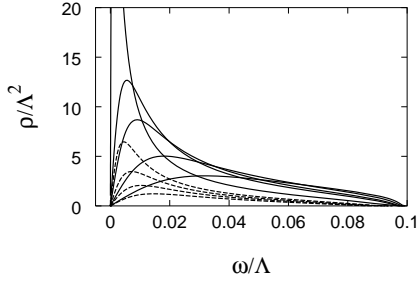
Fig. 3. Spectral function in the spacelike momentum region with $|\boldsymbol{q}|/\Lambda = 0.1$, $T = T_c$ and $m/\Lambda = 0.01$ for several μ (see text).
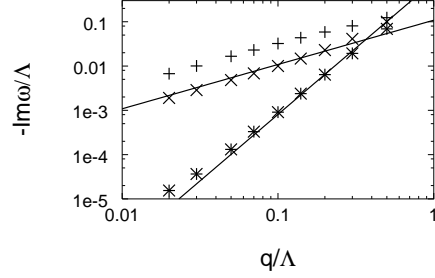
Fig. 4. The pole position of $\chi_{mm}(\omega, \boldsymbol{q})$ as a function of $|\boldsymbol{q}|/\Lambda$ for $\mu/\Lambda = 0.56$ ($\times$), μ_c/Λ ($*$), 0.58 (+).

$E_{\boldsymbol{k}+\boldsymbol{q}} - E_{\boldsymbol{k}} \sim \boldsymbol{v} \cdot \boldsymbol{q}$. The peak is strongly enhanced as compared with the free gas spectrum shown in the dashed line in Fig. 2 (a). The enhancement of this spectrum is demonstrated for μ/Λ=0.58, 0.575, 0.572, 0.571, 0.5701=μ_c/Λ (solid lines), 0.5682, 0.5652, 0.56, 0.55 (dashed lines) with fixed temperature $T_c/\Lambda = 0.19485$ in Fig. 3.

We found numerically a pole of $\chi_{mm}(\omega, \boldsymbol{q})$ on the negative imaginary axis of ω, which we expect is associated with this spectral enhancement. In fact, we confirmed that near CEP $\chi_{mm}(\omega, \boldsymbol{q})$ is well described with this single pole as

$$\chi_{mm}(\omega, \boldsymbol{q}) \sim \frac{1}{-i\frac{\omega}{\lambda(\boldsymbol{q})} + \chi_{mm}^{-1}(\boldsymbol{q})} = \frac{\lambda(\boldsymbol{q})}{-i\omega + \omega_c(\boldsymbol{q})} \qquad (3\cdot 3)$$

with $\lambda(\boldsymbol{q}) \propto |\boldsymbol{q}|$ and $\omega_c(\boldsymbol{q}) = \lambda(\boldsymbol{q})\chi_{mm}^{-1}(\boldsymbol{q})$. We note that $\omega_c(\boldsymbol{q}) \propto |\boldsymbol{q}|$ in the non–critical case while $\omega_c(\boldsymbol{q}) \propto |\boldsymbol{q}|^3$ at CEP because $\chi_{mm}^{-1}(\boldsymbol{q}) \propto \boldsymbol{q}^2$ there (see Fig. 4).

In the NJL model the singularity of the baryon number susceptibility $\chi_{\mu\mu}$ at CEP can be generated again by the denominator in (3·2). It is noteworthy that only the p–h collective mode can mix with $\chi_{\mu\mu}$ through the coupling because $\Pi_{m\mu}(\omega > 0, \boldsymbol{0}) = 0$. The importance of the mode with the hydrodynamic character is consistent with the argument given in §2.

We conclude that the origin of the divergences at CEP is the softening of this p–h spectrum in the NJL model. We think that the essence of this understanding still remain valid after the inclusion of the critical fluctuations beyond the mean field approximation although these effects are to be elaborated. If confinement is treated, the p–h spectrum may come from the nucleons.

3.3. *Spectral contribution along the critical line* [12)]

Now that we know the dominance of the p–h mode in χ_{mm} at CEP, let us examine its contribution in the chiral transition with $m = 0$ because the p–h mode always exists in medium. We define ratio R by

$$R = \frac{\chi_{mm}(0, \boldsymbol{0}^+) - \chi_{mm}(0^+, \boldsymbol{0})}{\chi_{mm}(0, \boldsymbol{0}^+)}, \qquad (3\cdot 4)$$

which measures the importance of the hydrodynamic spectrum as explained in §2. This ratio for $\chi_{\mu\mu}$ is always unity due to the spectral property of the conserved
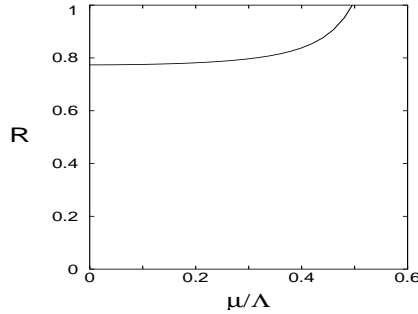
Fig. 5. Ratio R along the critical line.

quantity. In Fig. 5, we present the ratio R of the scalar channel along the critical line approached from the broken phase (see also Fig. 1). It might be a little surprise that the p–h mode spectrum gives a finite fraction of the critical divergence even in the second–order chiral transition, and it finally dominates the spectral sum ($R = 1$) at TCP, where $\chi_{\mu\mu}$ and χ_{TT} diverge in addition to χ_{mm}. This result seems natural from the argument given in §2.

If the critical line is approached from the symmetric phase, on the other hand, the p–h collective spectrum does not contribute to χ_{mm}. Thus the divergence solely comes from the sigma meson mode ($R = 0$) and $\chi_{\mu\mu} = \Pi_{\mu\mu}(0, \mathbf{0}^+)$. Actually there is no p–h spectral strength in the scalar channel at $\boldsymbol{q} = 0$ in the symmetric phase. This is understood as follows: the absorption amplitude of the collective mode with momentum $\boldsymbol{q}$ by a quark $q_L(\boldsymbol{k})$ is proportional to a spinor product $\bar{u}_R(\boldsymbol{k}+\boldsymbol{q})u_L(\boldsymbol{k}) \propto |\boldsymbol{q}|$ with a helicity flip. (Since a massive quark with a definite chirality has both helicity components, the helicity flip is unnecessary in the broken phase.)

§4. Time–dependent Ginzburg–Landau approach [12]

In order to confirm the generality of our result, let us repeat our analysis within the TDGL approach here. It is essential to introduce another density φ [10] near TCP which is physically a linear combination of the baryon number and the energy densities, and whose susceptibility diverges at TCP (and at CEP as well). We expand the GL effective potential in terms of the ordering densities σ and φ around TCP as

$$\Omega = \int d^3x \left(\frac{\kappa}{2}(\nabla\sigma)^2 + a_0\sigma^2 + b_0\sigma^4 + c\sigma^6 + \gamma\sigma^2\varphi + \frac{1}{2}\varphi^2 - h\sigma - j\varphi \right). \qquad (4\cdot1)$$

Coupling between σ and φ must respect the underlying chiral symmetry. Eliminating the density φ by $\partial\Omega/\partial\varphi = \gamma\sigma^2 + \varphi - j = 0$, we recover the usual σ^6 theory of the free energy with σ^2 and σ^4 coefficients replaced by $a = a_0 + \gamma j$ and $b = b_0 - \frac{1}{2}\gamma^2$.

In the TDGL approach the coefficients are unknown. In Fig. 6 shown are the typical examples of the three–phase coexistence ((a), (b)) and the CEP ((c), (d)). In case of exact chiral symmetry ($h = 0$), the σ direction is obviously special. Although the GL potential of single order parameter σ becomes flat at CEP, the actual flat direction is a linear combination of σ and φ. Both the scalar susceptibility $\chi_h =$
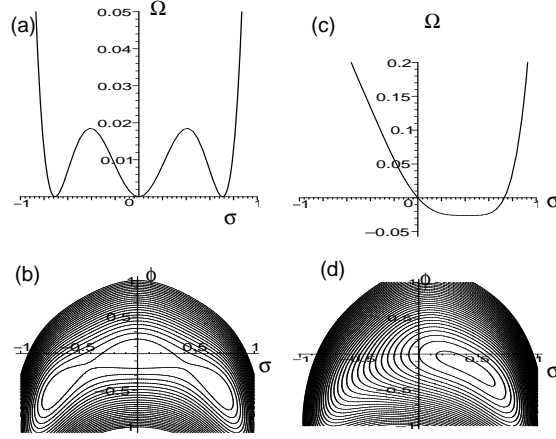
Fig. 6.   Schematic GL potentials at a three–phase coexisting point ((a) and (b)) and at a CEP ((c) and (d)), with single ordering density (upper) and with two ordering densities (lower).

$1/(2a + 12b\sigma^2 + 30c\sigma^4)$ and the φ–susceptibility $\chi_j = 1 + 4\gamma^2\sigma^2\chi_h$ diverge there. We stress here that once $h \neq 0$ one may equally use an alternative GL potential with single order parameter φ defined by eliminating σ in favor of φ in Eq. $(4\cdot1)$ [12].

Differently from the NJL case where the collective modes are generated by the microscopic interaction and then coupled with the scalar and vector channels, the dynamics here in the TDGL approach is introduced phenomenologically from the outset [10] via

$$L_\sigma(i\partial_t)\sigma = -\frac{\delta\Omega}{\delta\sigma}, \quad L_\varphi(i\partial_t)\varphi = -\frac{\delta\Omega}{\delta\varphi}. \qquad (4\cdot2)$$

One stringent condition on the time dependence is that the density φ is a conserved quantity, and possible form of L_φ will be of diffusion $L_\varphi(\omega) = -i\omega/\lambda\boldsymbol{q}^2$ or sound–like $L_\varphi(\omega) = -\omega^2/\lambda\boldsymbol{q}^2$. On the other hand, it is natural to expect $L_\sigma(\omega) = -\omega^2/\Gamma$ (propagation) or $-i\omega/\Gamma$ (relaxation). Here we assume coefficients λ, Γ are constant.

By linearizing the equation of motion around the equilibrium densities, we obtain the condition for the normal mode

$$\det\begin{pmatrix} L_\sigma(i\partial_t) + \Omega_{\sigma\sigma} & \Omega_{\sigma\varphi} \\ \Omega_{\sigma\varphi} & L_\varphi(i\partial_t) + \Omega_{\varphi\varphi} \end{pmatrix} = 0, \qquad (4\cdot3)$$

where $\Omega_{ab} = \delta^2\Omega/\delta a\delta b|_{\mathrm{eq}}$. Because of the soft nature of the conserved densities, the solution for the mixing between (*e.g.,*) the propagation and the diffusion is found in the small–$\boldsymbol{q}^2$ limit as

$$\frac{-\omega^2}{\Gamma} = -(\chi_h^{-1} + 4\gamma^2\sigma^2), \quad \frac{-i\omega}{\lambda\boldsymbol{q}^2} = -\chi_j^{-1}. \qquad (4\cdot4)$$

The soft mode becomes softer in the mixing among the modes, and the normal mode with diffusion–like character shows the critical slowing ($\propto \chi_j^{-1} \to 0$) while the propagating mode does not at CEP ($\sigma \neq 0$).

The response function is the inverse of Eq. (4·3) with the retarded boundary condition. Using the spectral function we can again discuss the mode contributions to the susceptibilities. For the scalar channel, the response function yields

$$\chi_h(\omega, \boldsymbol{q}) = \frac{L_\varphi(\omega) + \Omega_{\varphi\varphi\boldsymbol{q}}}{(L_\sigma(\omega + i\varepsilon) + \Omega_{\sigma\sigma\boldsymbol{q}})(L_\varphi(\omega) + \Omega_{\varphi\varphi\boldsymbol{q}}) - \Omega_{\sigma\varphi\boldsymbol{q}}^2}. \tag{4·5}$$

The susceptibility $\chi_h = \lim_{\boldsymbol{q}\to 0}\chi_h(0, \boldsymbol{q})$ is expressed as a spectral sum of the two modes as

$$\chi_h = \chi_h\left(\frac{\chi_h^{-1}}{\chi_h^{-1} + 4\gamma^2\sigma^2} + \frac{4\gamma^2\sigma^2}{\chi_h^{-1} + 4\gamma^2\sigma^2}\right), \tag{4·6}$$

where the first term in the bracket is from the propagating mode and the second from the diffusion–like mode in Eq. (4·4). From this simple expression we find that in the chirally symmetric phase ($\sigma = 0$) there is no contribution from the diffusion mode $R = 0$. In the second order chiral transition approached from the broken phase, a finite fraction of the divergence comes from the diffusion–like mode ($0 < R < 1$), and $R = 1$ at TCP. In the criticality of CEP the diffusion–like mode saturates the divergence ($R = 1$) because $\chi_h^{-1} = 0$ and $\sigma \neq 0$. Incidentally, in the ω–limit the diffusion–like contribution drops out due to its hydrodynamic nature. These discussions are completely in parallel to the NJL case, and consistent with the argument in §2.

Acknowledgments

References

1) Z. Fodor and S.D. Katz, JHEP 0203 (2002), 014, and see contributions in these proceedings for recent developments.
2) M. Asakawa and K. Yazaki, Nucl. Phys. **A504** (1989), 668.
3) S. Gavin, A. Gocksch, R.D. Pisarski, Phys. Rev. D **49** (1994), 3079.
4) J. Berges and K. Rajagopal, Nucl. Phys. **B538** (1999), 215.
5) M.A. Halasz, A.D. Jackson, R.E. Shrock, M.A. Stephanov, and J.J.M. Verbaarschot, Phys. Rev. D **58** (1998), 096007.
6) M.A. Stephanov, in these proceedings, and references therein.
7) M.A. Stephanov, K. Rajagopal and E.V. Shuryak, Phys. Rev. Lett. **81** (1998), 4816.
8) M.A. Stephanov, K. Rajagopal and E.V. Shuryak, Phys. Rev. D **60** (1999), 114028.
9) B. Berdnikov and K. Rajagopal, Phys. Rev. D **61** (2000), 105017.
10) P.C. Hohenberg and B.I. Halperin, Rev. Mod. Phys. **49** (1977), 435.
11) H. Fujii, Phys. Rev. D **67** (2003), 094018.
12) H. Fujii and M. Ohtani, in preparation.
13) Y. Hatta and T. Ikeda, Phys. Rev. D **67** (2003), 014028.
14) M. Harada, in these proceedings.
15) T. Hatsuda and T. Kunihiro, Phys. Rev. Lett. **55** (1985), 158.
16) T. Hatsuda and T. Kunihiro, Phys. Rep. **247** (1994), 221.
17) P. Chakraborty, M.G. Mustafa, M.H. Thoma, Phys. Rev. D **68** (2003), 085012.